Eur Biophys J (1996) 24: 117–124

European Biophysics Journal

Low temperature optical spectroscopy of low-spin ferric hemeproteins

Maurizio Leone, Antonio Cupane, Lorenzo Cordone

Istituto di Fisica dell'Università di Palermo and GNSM-INFM, Via Archirafi 36, I-90123 Palermo, Italy

Received: 24 January 1995 / Accepted in revised form: 18 October 1995

Abstract. We report the Soret absorption spectra (500-350 nm) of the cyanomet derivatives of human hemoglobin and horse myoglobin, in the temperature range 300-20 K and in two different solvents (65% v/v glycerol-water or 65% v/v ethylene glycol-water). In order to obtain information on stereodynamic properties of active site of the two hemeproteins, we perform an analysis of the band profiles within the framework of electron-vibrations coupling. This approach enables us to single out the various contributions to the spectral bandwidth, such as those arising from non-radiative decay of the excited electronic state (homogeneous broadening) and from the coupling of the electronic transition i) with high frequency modes (that determines the vibronic structure of the band) and ii) with a "bath" of low frequency modes (that is responsible for the temperature dependence of the experimental spectra). We discuss the relevant parameters and their temperature dependence and compare them with the ones already reported for other derivatives of the same hemeproteins in the same solvents. In particular, non-harmonic contributions to soft modes are found, for cyanomet derivatives, to be larger than those observed for liganded carbonmonoxy but smaller than those observed for unliganded deoxy derivatives. The reported data enable us to obtain information on the dependence of stereodynamic properties of the heme pocket upon iron oxidation state, dimensions of the exogenous ligand and composition of the external matrix.

Key words: Protein dynamics – Optical spectroscopy

Introduction

The optical absorption spectra of heme proteins depend markedly on temperature; the physical origin of this effect can be traced on the coupling of the electronic transitions responsible for the absorption bands with the thermal motions of the neighboring atoms. Accurate optical absorption measurements performed from room temperature to 20 K, together with a suitable data analysis, can therefore give relevant information on the dynamic properties of the protein in the proximity of the chromophore.

In the case of the Soret band of heme proteins, owing to the large extinction coefficient, electron-vibrations interactions can be fairly well described within the Franck-Condon approximation and a non-heuristic deconvolution of the band profiles at various temperatures has been reported (Cupane et al. 1993a, 1995; Shomacker and Champion 1986; Srajer and Champion 1991). In this way the various contributions to the overall bandwidth (such as homogeneous broadening due to the finite lifetime of the excited state, vibronic coupling with high frequency nuclear vibrations, Gaussian broadening due to the coupling with a "bath" of low frequency modes, inhomogeneous broadening due to conformational heterogeneity) can be singled out and their temperature dependence can be studied.

This approach has been exploited in the last few years to study the dynamic properties of both the CO-liganded and unliganded derivatives of various hemeproteins and heme complexes (Boffi et al. 1994; Cordone et al. 1986, 1988, 1990; Cupane et al. 1988, 1993a, b, 1995; Di Pace et al. 1992; Leone et al. 1987, 1992, 1994). In particular, an increase of the Gaussian line broadening well above the predictions of the harmonic approximation has been observed at high temperatures. This effect, that has been attributed to the onset of anharmonic contributions to low frequency modes, depends significantly upon the particular protein investigated and upon its state of ligation but much less upon the composition of the external medium (Boffi et al. 1994; Cupane et al. 1993a, b; Di Pace et al. 1992; Leone et al. 1994).

In this paper we report the temperature dependence of the Soret band of cyanomet hemoglobin (HbCN) and cyanomet horse myoglobin (HoMbCN) in two different solvents (65% v/v glycerol or ethylene glycol in water). The interest in studying CN-liganded derivatives in compari-

Correspondence to: M. Leone

son with the CO-liganded and the deoxy ones stems also from the fact that, owing to its smaller linear dimensions (the C≡N distance is 1.16 Å, as compared to the C≡O distance of 1.43 Å), the CN^- ligand is known to bind more perpendicular to the heme plane than CO (Moffat et al. 1979). The aim of this work is to contribute towards the understanding of the role played by ligand dimensions, iron atom oxidation state and protein solvent interactions on the dynamic properties of the active site in hemeproteins.

Experimental

Samples

Hemoglobin was prepared from the blood of a single donor, as already described (Cordone et al. 1979). Oxyhemoglobin was oxidized by addition of a 4-fold molar excess of potassium ferricyanide; excess ferricyanide and ferrocyanides were removed by dialysis. Ferric myoglobin (from horse skeletal muscle) purchased from Sigma was dissolved in 0.1 M phosphate buffer pH 7 and centrifuged to remove any precipitate; to ensure complete oxidation, addition of potassium ferricyanide and dialysis was also performed. The cyanomet forms of both proteins were obtained by addition of 10^{-3} M KCN. Samples for spectrophotometric measurements contained 65% v/v cryoprotectant (glycerol or ethylene glycol) in water, 0.1 M phosphate buffer ($KH_2PO_4 + K_2HPO_4$, pH = 7 in water at room temperature) and approximately 4×10^{-6} M (in heme) protein.

Optical spectroscopy

Absorption spectra (500-350 nm) were measured with a Jasco Uvidec 650 spectrophotometer, set to 0.4 nm bandwidth, 1 sec integration time and 40 nm/min scan speed; data were recorded at 0.4 nm intervals. The experimental setup for the optical measurement has been already reported (Cordone et al. 1986); samples remained homogeneous and transparent in the whole temperature range and no cracking occurred.

The baseline recorded at room temperature with the same cuvette used for the measurements and filled with the water-cosolvent-buffer mixture used for diluting the proteins under investigation was subtracted from the spectra measured at various temperatures; indeed, in the spectral region of interest, the baseline has been shown not to depend upon temperature (Cordone et al. 1986). Moreover, the absorbance at 490 nm, which corresponds to the minimum in the spectra of both metHbCN and metMbCN, was brought to a zero value for all the spectra; this appoximation does not significantly influence the analysis, since the absorbance at 490 nm (which results mainly from the high frequency tail of Q_o/Q_v band) is about 0.03 (and temperature independent), in our measurements, as compared to the 0.6 ÷ 1.0 value of the Soret band maximum.

Data analysis

Spectral deconvolutions were performed on a Microway I860 add-on board for IBM-PC (Microway Europe Ltd., Kingston upon Thames, GB); the mean square deviation (χ^2) was minimized using a non linear least-squares algorithm (Marquardt 1963). Errors on fitting parameters were calculated by inversion of the curvature matrix, within the approximation of parabolic χ^2 hyper-surface around the minimum; they correspond to 67% confidence limits (Bevington and Robinson 1992).

An analytical expression for the Soret band profile at various temperatures is obtained by considering a single electronic transition coupled with several harmonic, Franck-Condon active, vibrational modes and treating the system within the Born-Oppenheimer and Condon approximations. Details on the theoretical approach used have been given in previous publications (Di Pace et al. 1992; Cupane et al. 1993a, 1994). Here we only report a short summary.

The absorbance at frequency v can be written as a Voigtian function:

$$A(v) = M v \left\{ \sum_{\{m_i\}}^{\infty} \left[\prod_i^{N_h} \frac{S_i^{m_i} e^{-S_i}}{m_i!} \right] \times \frac{\Gamma}{\left[v - v_0(T) - \sum_i^{N_h} m_i R_i v_i(g) \right]^2 + \Gamma^2} \times \frac{1}{\sigma(T)} e^{-\frac{v^2}{2\sigma^2(T)}} \right\} \quad (1)$$

where M is a constant proportional to the square of the electric dipole moment and Γ is the damping factor related to the finite lifetime of the excited state (homogeneous broadening). The product extends to all high-frequency vibrational modes (i.e. with $hv_i \gg k_B T$) coupled to the electronic transition and the summations to their occupation numbers; Moreover v_i, S_i and R_i are respectively the frequency, linear and quadratic coupling constants for the i-th high frequency mode. The symbol ⊗ indicates the convolution operator. Coupling of the electronic transition with a bath of low-frequency modes (i.e. with frequency smaller than the observed bandwidth) is treated within the "short times approximation" (Chan and Page 1983); this brings about the convolution with a Gaussian lineshape and contributes the temperature dependent terms $\sigma^2(T)$ and $v_0(T)$ to the linewidth and peak position of the band respectively.

The analysis of the Soret absorption spectra of cyanide derivatives is based on fittings of the experimental data to (1). The fitting parameters are M, Γ, S_i, $\sigma(T)$ and $v_0(T)$. v_i values relative to high frequency modes are taken from resonance Raman (RR) spectra reported in the literature

(Desbois et al. 1979; Asher 1981). The most coupled modes are those at 365, 676 and 1374 cm^{-1}, while other less coupled modes do not contribute significantly to the lineshapes and are therefore neglected. It is worth mentioning that in RR spectra of heme-proteins 676 cm^{-1} and 1375 cm^{-1} correspond to very sharp lines and are thought to arise from in-plane vibrational modes of the heme group, i.e. ν_7 mainly $C_\alpha N$ stretch, $C_\alpha C_m C_\alpha$ and $C_\alpha C_m H$ bending and ν_4 mainly $C_\alpha N$ stretch, $C_\alpha C_\beta$ stretch and $C_\alpha C_m H$ bending, respectively (Li et al. 1990). In contrast, 365 cm^{-1} is an "average effective" frequency accounting for several quasi degenerate peaks; both in-plane and out-of-plane modes contribute to this spectral region. We also attempted to include in the fittings coupling to the 1100 cm^{-1} mode, but the resulting linear coupling strength turned out to be smaller than 0.01: coupling with this mode was therefore neglected. Parameters S_i were determined from the low temperature spectra and kept fixed in the analysis of the spectra recorded at all the temperatures. Temperature independent S_i values are in agreement with previous reports (Cupane et al. 1993a; Di Pace et al. 1992; Schomacker and Champion 1986). Parameter Γ is also determined from the low temperature spectra and kept fixed in the analysis of the spectra recorded at all temperatures. The temperature behavior of parameter Γ for CO and deoxy hemeproteins has been discussed in detail in previous publications (Di Pace et al. 1992; Cupane et al. 1993). In these cases Γ is unambiguously determined by the red edges of the bands at all temperatures, and it does not vary in the whole temperature range investigated, with the exception of MbCO (Di Pace et al. 1992). In the present case of MbCN and HbCN the determination of Γ is more cumbersome, in view of the presence of the small extra band at 22,500 cm^{-1} that makes the red edge less sharp, especially at high temperature. We stress, however, that fitting of the band profile, performed without constraints, results in a more noisy thermal behavior of the relevant parameters without systematic effects.

Within the harmonic approximation the analytical expression of $\sigma^2(T)$ mand $\nu_0(T)$ are given by:

$$\nu_0(T) = \nu_{00} - 1/4\, N\langle\nu\rangle(1-R)\coth(h\langle\nu\rangle/2kT) + C \quad (2)$$

$$\sigma^2(T) = NSR^2\langle\nu\rangle^2 \coth(h\langle\nu\rangle/2kT) + \sigma_{in}^2 \quad (3)$$

In (2) and (3) $\langle\nu\rangle$, S and R are the effective frequency, linear and quadratic coupling constants of the low frequency bath, N is the number of soft modes, ν_{00} is the frequency of the purely electronic (0–0) transition, and C takes into account other temperature independent contributions to the peak position of the band. The term σ_{in}^2 in (3) takes into account the inhomogeneous broadening of the Soret band arising from different conformational substates and heme environments (Frauenfelder et al. 1988); in fact for the cyanomet derivatives, owing to the in plane position of the iron atom, such effects can be modeled as a Gaussian distribution of purely electronic transition frequencies (ν_{00}), thus contributing an additional temperature independent term (σ_{in}) to the width of the Gaussian component of the Voigtian in (1).

Results and discussion

In Fig. 1a we report the Soret band of HoMbCN at various temperatures. Spectra consist of a main band, centered at about 420 nm, attributed to a $\pi \rightarrow \pi^*$ electronic transition (B band) (Eaton et al. 1978; Eaton and Hofrichter 1981). By lowering the temperature, narrowing and peak position shift occur, to an extent which depends on the particular protein and on the solvent conditions. To show these effects more clearly we report normalized spectra for HbCN at T = 300 and 20 K in Fig. 1b. An inspection of the raw data in Fig. 1a also shows a less intense band on the blue side, attributed to a different $\pi \rightarrow \pi^*$ electronic transition (N band), and a shoulder on the red side of the spectra. This shoulder, clearly resolved at cryogenic temperatures, is almost undetectable at room temperature, owing to broadening of the bands; moreover, it is observed for both hemoglobin and myoglobin in both solvents used. A z-polarized band near 20,500 cm^{-1} has been reported by Makinen and Churg (1983) in the optical spectra of met MbCN; this band was attributed to a porphyrin $a_{2u}(\pi) \rightarrow a_{1g}(dz^2)$ orbital promotion, in good agreement with the theoretical prediction of 21,000 cm^{-1}. Moreover, several spin-allowed transitions are expected for a low-spin Fe(III) ion; although precise values for the crystal field parameters in met HbCn and met MbCN are not available, these $d \rightarrow d$ transitions are expected to be near 22,000 cm^{-1}. We tend to exclude the possibility that this shoulder is due to a Soret sub-band, arising from distinct conformational substates, in view of the large frequency shift ($\approx$2,000 cm^{-1}).

To take into account this shoulder a Gaussian component has been added to the theoretical band profile (Eq. 1);

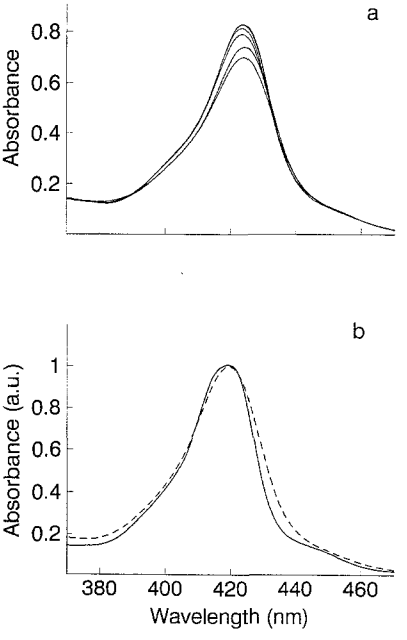

Fig. 1. **a** Soret band of HoMbCN at various temperatures in 65% ethylene glycol/water; the arrows indicate the direction of spectral changes observed on lowering the temperature. **b** Normalized spectra at 300 K (*dashed line*) and 20 K (*continuous line*) of HbCN in the same solvent conditions

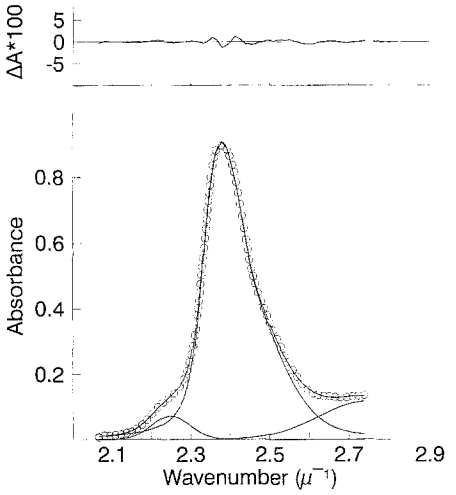

Fig. 2. Deconvolution of the 20 K spectrum of HbCN in 65% glycerol/water in terms of (1). Circles are the experimental points; continuous lines represent the Soret band fitted in terms of Eq. (1), the contributions from the higher frequency N band and from the lower frequency band (see text), and the overall synthesized band profile. For figure readability not all the experimental points are included. The residuals are also reported in the upper panel, on an expanded scale

moreover, in view of its smallness and in order to avoid fitting ambiguities arising from an excessive number of adjustable parameters, the peak frequency and width of this Gaussian component have been held fixed to 22,500 and 480 cm^{-1} respectively. The spectra at various temperatures are therefore deconvoluted in terms of a Voigtian (Eq. 1) plus two Gaussian components which account for the two lateral bands. A typical fitting is reported in Fig. 2, together with the residuals on an expanded scale; we stress that fittings of similar quality are obtained for all the experimental spectra at all temperatures.

In Table 1 we report the values of parameters Γ and S_i (i.e. of the homogeneous bandwidth and of the linear coupling constants with high frequency vibrational modes) obtained from the fittings, in comparison with analogous quantities previously found for carbonmonoxy and deoxy derivatives of the same proteins; only data referring to 65% glycerol/water solutions are reported since no sizeable solvent effect is observed for these quantities. Data in Table 1 show that cyanomet derivatives are characterized by values of the linear coupling constants to the 676 cm^{-1} mode similar to those obtained for the other two derivatives, while an increase is observed for the S values relative to the 1374 and 365 cm^{-1} modes; in particular, the coupling constant of the 365 cm^{-1} mode appears rather large. In this respect we stress the following points:

1) From the reported S_{365} values one would expect a rather strong increase of the resonance Raman intensity in the region 300–400 cm^{-1}. The resonance Raman spectra of HbCN and MbCN have been measured by Desbois et al. (1979) and such an increase is not so clear from their data. However, these experiments were performed with 441.6 nm excitation, which is far from resonance with the Soret band ($\lambda_{max} \approx 425$ nm). Accurate Raman excitation profiles measurements of the low frequency modes would be needed to clarify this point.

2) Rather strong coupling ($S \sim 1$) with a mode at about 365 cm^{-1} have also been observed for the four charge transfer transitions which characterize the near infrared spectrum of the same ferric cyanomet derivatives (Leone et al. 1992).

3) Since our resolution of the vibronic structure is limited by the intrinsic homogeneous width of the band, i.e. 230 cm^{-1}, the above "high frequency" modes are to be considered as effective ones, averaging over the nearby frequency region. This could explain the rather large S values reported. A similar approach has been followed by Champion and coworkers (Shomacker et al. 1984) in a study of Raman scattering of ferrous and ferric cytochrome-C; these authors find a cluster of Raman active modes between 300 and 500 cm^{-1}, that they treat as a single average mode at 390 cm^{-1}, whose mean coupling constant is about 0.2 and increases upon oxidation.

4) An increase of the Raman scattering intensity in the region around 400 cm^{-1} with respect to that around 674 cm^{-1} is observed, for cytochrome-C, upon iron oxidation (Shomacker et al. 1984). This increase is in agreement (although less pronounced) with the S_{365}/S_{674} increase for cyanomet derivatives reported in Table 1.

5) A further possibility is that the S_{365} values reported in Table 1 are overestimated owing to the presence of Soret sub-bands arising from optically distinguishable conformers of the hemegroup with a peak frequency shift of the order of 350 cm^{-1} (Gilch et al. 1993, 1994). We therefore

Table 1. Low temperature (T = 20 K) linear coupling constants of the high frequency modes and Γ values for Hb-CN and Mb-CN, in 65% v/v glycerol aqueous solutions. As reported in the text, no appreciable solvent dependence of fitting parameters was found. The values of the fitting parameters relative to carbonmonoxy and deoxy derivatives of the same proteins are also reported for comparison (Boffi et al. 1994; Cupane et al. 1993a, b; Di Pace et al. 1991)

	S_{365}	S_{676}	S_{1100}	S_{1374}	Γ/cm^{-1}
Hb-CN	0.95±0.01	0.14±0.01	<0.01	0.15±0.01	230±10
Hb-CO[a]	0.05±0.01	0.07±0.01	0.02±0.01	0.08±0.01	215± 4
Hb[b]	0.11±0.02	0.21±0.02	<0.01	0.05±0.01	175± 9
Mb-CN	0.79±0.05	0.13±0.01	<0.01	0.18±0.01	230±10
Mb-CO[a]	0.10±0.01	0.06±0.01	0.02±0.01	0.09±0.01	213± 8
Mb[b]	0.36±0.03	0.25±0.02	<0.01	0.10±0.01	170±10

[a] S values for carbonmonoxy derivatives refer to the high frequency mode at 350, 676, 1100, 1374 cm^{-1} respectively
[b] S values for deoxy derivatives refer to the high frequncy mode at 370, 674, 1100 and 1357 cm^{-1} respectively

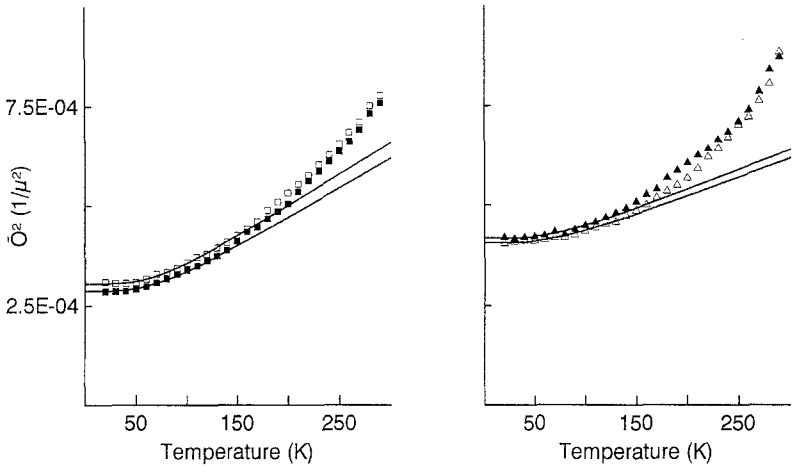

Fig. 3. Temperature dependence of parameter σ^2 for HbCN (*left panel, squares*) and HoMbCN (*right panel, triangles*); full symbols refer to samples in 65% ethylene glycol/water, open symbol to samples in 65% glycerol/water. The continuous lines represent fittings of the data in terms of (3); fitting ranges are 20–140 K for samples in ethylene glycol/water and 20–160 K for samples in glycerol/water

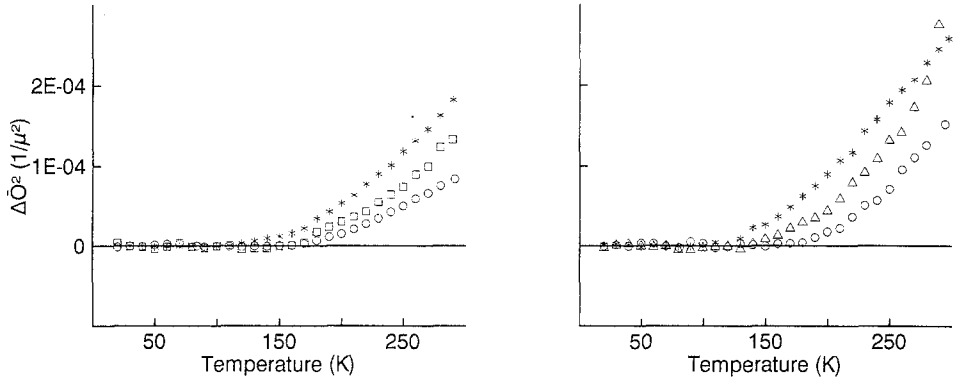

Fig. 4. $\Delta\sigma^2$ values for Hb (*left panel*) and Mb derivatives (*right panel*) in 65% ethylene glycol/water solutions. *Asterisks:* deoxy derivatives; *squares:* cyanomet derivatives; *circles:* carbonmonoxy derivatives

performed a deconvolution of the spectra in terms of two Voigtian sublines shifted by 350 cm^{-1} having the same Γ and σ values. In this fitting the S_{365} value dropped to about 0.5 (without significant variations of S_{674} and S_{1374}) while the temperature dependence of σ^2 and v_0 (Eq. 1) remained unchanged.

The thermal behavior of σ^2 values for both proteins studied and in both solvent conditions is reported in Fig. 3. A first inspection of the data reported in Fig. 3 shows that solvent effects are small and that σ^2 values obey the behavior predicted by (3) only in a limited temperature range (20 K < T < 160 K). An unambiguous indication of this last behavior arises from the fact that for $T \to \infty$ Eq. (3) results in an expression, linear in T, whose extrapolation to 0 K gives σ^2_{in} (i.e. either positive or zero values). In contrast, the linear extrapolation to 0 K of the high temperature σ^2 values gives a negative intercept, thus implying a negative, non physical, inhomogeneous broadening. Physically meaningful fittings in terms of (3) can be performed up to ≈160 K; the continuous lines reported in Fig. 3 represent such fittings. Values of the relevant parameters are reported in Table 2, in comparison with the analogous quantities for deoxy and carbonmonoxy derivatives: for cyanomet derivatives enhanced coupling with the bath of low frequency modes and larger σ_{in} values are found. Since Eq. (3) is obtained within the harmonic approximation, we attribute the anomalous σ^2 increase at high temperatures on the onset of anharmonic contributions to nuclear motions. In order to evaluate it, in Fig. 4 we report $\Delta\sigma^2$ values (i.e. the differences between experimental σ^2 values and the continuous lines in Fig. 3), together with the same quantities already found for deoxy and carbonmonoxy derivatives; only data relative to 65% glycerol/water solutions are reported, since no sizeable solvent effects are evident.

Leone et al. (1994) have shown that, in the case of hemeproteins and heme complexes, anharmonic contributions to σ^2 arise from motions of the iron with respect to the heme plane. Indeed, one can argue that after melting of the solvent medium at the glass tansition, the release of the constraints imposed by the proteo-solvent matrix enables porphyrin-iron-ligand motions of amplitude larger than that expected from the low temperature behavior. In the case of hemeproteins, the above motions may well be driven by molecular motions within the protein matrix via the iron-proximal histidine bond and/or via various non covalent heme-ligand-protein interactions; anharmonic contributions may therefore also reflect interconversion between substates that causes a temperature dependence of the parameter σ_{in}.

The relevance of iron-porphyrin vibrations to the low temperature σ^2 thermal behavior is also pointed out by a recent normal mode analysis of MbCO with 170 water molecules (Melchers et al. unpublished results): in fact, the iron mean square fluctuations calculated with respect

Table 2. Values of the parameters obtained by fitting the v_0 ad σ^2 behavior in terms of (2) and (3). Fittings were performed from 20 K to the temperature of the glass transition of the solvent, i.e. 140 K for ethylene glycol and 160 K for glycerol aqueous solutions. The analogous quantities for carbonmonoxy and deoxy derivatives of the same proteins in 65% glycerol/water solutions are also reported for comparison (Boffi et al. 1994; Cupane et al. 1993a, b; Di Pace et al. 1991)

	NS[a]	$\langle v \rangle / cm^{-1}$	R[b]	$(v_{00}+C)/cm^{-1}$	σ_{in}/cm^{-1}
Hb-CN [Et-Gly]	0.8±0.1	140±20	0.991±0.006	23,553±6	114± 9
Hb-CN [Glyc]	0.9±0.1	140±18	0.988±0.005	23,535±8	117± 9
Hb-CO [Glyc]	0.5±0.2	170±20	0.990±0.006	23,944±4	70±23
Hb [Glyc]	0.6±0.1	140±10	0.990±0.001	23,043±2	/[c]
Mb-CN [Et-Gly]	0.5±0.1	140±18	1.02 ±0.007	23,336±8	175± 7
Mb-CN [Glyc]	0.5±0.1	140±16	1.01 ±0.005	23,339±7	177± 8
Mb-CO [Glyc]	0.4±0.1	179±10	1.01 ±0.005	23,553±5	35±20
Mb [Glyc]	0.4±0.1	153±10	1.02 ±0.005	22,590±2	/[c]

[a] NS values were obtained under the assumption $R^2 \approx 1$

[b] The R values are obtained by assuming coupling with N = 50 low frequency modes

[c] For deoxy derivatives inhomogeneous broadening is due essentially to the iron position out of the mean heme plane, as revealed by the asymmetric Soret band lineshape; this effect is modeled as a non-Gaussian distribution of v_{00} transition frequencies and therefore by a further convolution of Eq. (1). For a deeper discussion, see Cupane et al. 1993 a, 1994

to the center of mass of the heme are in good agreement with the analogous values deduced from low temperature optical spectroscopy.

The coupling of out-of-plane iron-porphyrin-ligand motions with the essentially in plane $\pi \rightarrow \pi^*$ electronic transition responsible for the Soret band (which should be absent in D_{4h} symmetry) should not be considered surprising (Shelnutt et al. 1991; Craig et al. 1992) in view of the lowered symmetry of the system brought about, for example, by distortion from planarity, proximal and distal ligand tilting and non-symmetric surrounding of the heme pocket. The eventual effect of pseudo Jahn-Teller coupling between the electronic ground state of the porphyrin and low lying electronic states of the iron (Stavrov 1993) should also be considered.

From Fig. 4 we note that the magnitude of anharmonic contributions observed for cyanomet derivatives are larger than those for the carbonmonoxy structure but smaller than those for the deoxy derivatives: This can be related to the different steric hindrance of the exogenous ligand in the three derivatives. Indeed, anharmonic contributions are smallest for CO derivatives, wherein the bound CO molecule bridges the proximal with the distal side, intermediate for CN derivatives in agreement with the smaller size of the bound ligand, and largest for the deoxy derivatives wherein the distal to proximal connection due to the bound ligand is lacking; in this respect we think it relevant to mention that in deoxy derivatives the onset of non-harmonic contributions is at ≈110 K, i.e. at temperatures whereby the surrounding solvent is still a solid matrix (Cupane et al. 1993). The intermediate effect of CN is also in agreement with the fact that it binds more perpendicular to heme plane than the CO (Moffat et al. 1979).

The thermal behavior of v_0 values for both proteins studied and in both solvent conditions is reported in Fig. 5. In this case a large solvent effect is observed; in fact, v_0 values can be fit by (2) only up to ≈140 K and ≈160 K for samples in ethylene glycol/water or glycerol/water solutions respectively: these temperatures are very close to the glass transition temperature of the solvent matrix (Cordone et al. 1988). The continuous lines reported in Fig. 5 represent such fittings; values of the relevant parameters are reported in Table 2, in comparison with the analogous quantities for deoxy and carbonmonoxy derivatives. Data in Fig. 5 suggest that, besides the anharmonicity effects (which, as shown in Fig. 3 do not depend significantly upon solvent composition for the cyanomet derivatives) a second effect, likely linked to the physical state of the solvent matrix, influences the thermal behavior of parameter v_0. We trace the origin of this second effect to the quantity v_{00} appearing in (2). This quantity is essentially related to pure electronic transition frequency, i.e. it is a measure of the energy difference between excited and ground electronic states when the nuclei are at rest in their equilibrium positions. This energy difference can be influenced, for example, by the local mean electric field experienced by the chromophore and therefore by the local protein structure (Srajer and Champion 1991) and/or by the dielectric constant of the external medium (Jaffe' and Orchin 1970). By considering the heme within the heme pocket as a chromophore embedded in a continuous proteo-solvent matrix, one can in principle expect the changes induced in this matrix when the solvent undergoes the glass transition to be reflected into v_{00} values. The fact that no sizeable solvent effect is observed for S_i and σ^2 values implies that, at the glass transition, the frequencies of vibrational modes and their coupling constants to the electronic transition are not substantially altered. Similar effects, that are linked to the glass transition of the proteo-solvent matrix and influence the thermal behavior of parameter v_0 while leaving unaltered parameter σ^2, have already been observed for the visible bands of various heme proteins (Cordone et al. 1988; Di Iorio et al. 1991) and for the IR stretching bands of a bound CO molecule in carbonmonoxy-myoglobin (Ansari et al. 1987).

The observation that, in the "harmonic" region, v_0 values relative to HbCN red-shift on increasing the temperature while for HoMbCN v_0 values blue-shift can be explained by considering that in Eq. (2) the quadratic coupling constant R, defined as the square ratio between

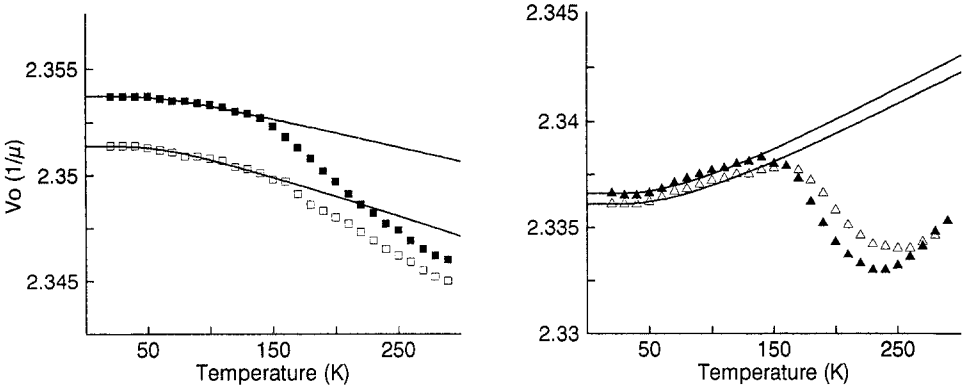

Fig. 5. Temperature dependence of parameter v_0 for HbCN (*left panel, squares*) and HoMbCN (*right panel, triangles*); full symbols refer to samples in 65% ethylene glycol/water, open symbols to samples in 65% glycerol/water. The continuous lines represent fittings of the data in terms of (2); fitting ranges are 20–140 K for samples in ethylene glycol/water and 20–160 K for samples in glycerol/water

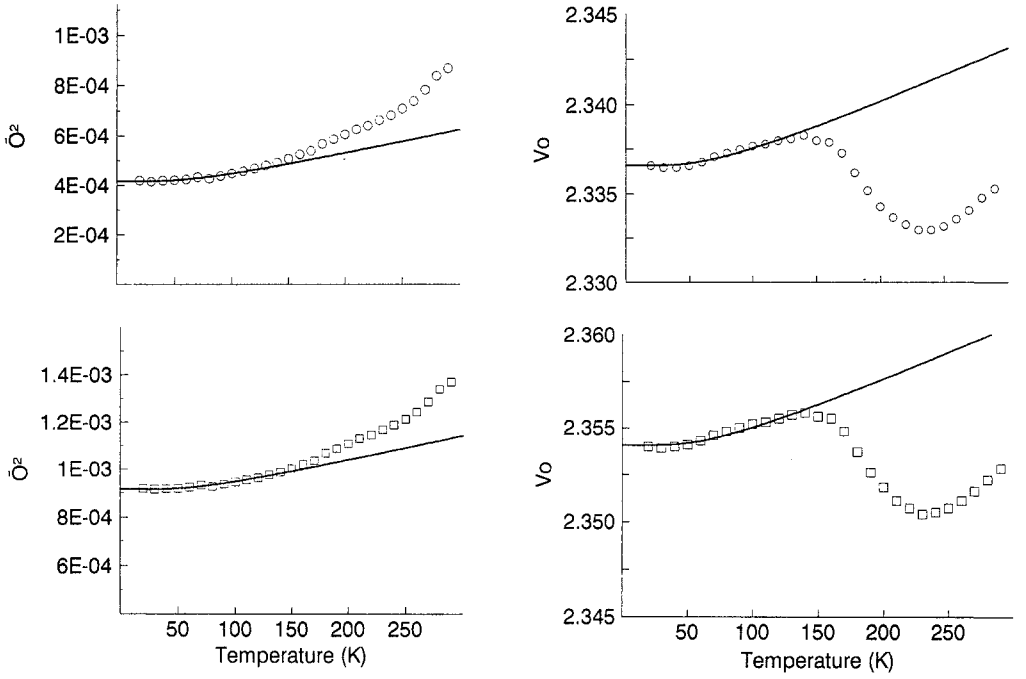

Fig. 6. Comparison between temperature dependence of parameters σ^2 (*left panels*) and v_0 (*right panels*) resulting from different fittings of the spectra of HoMbCN in ethylene glycol/water (see text). Circles (*upper panels*) refer to the fitting procedure outlined in the Data Analysis section (see also Figs. 3 and 5); squares (*lower panels*) refer to an analysis which does not explicitly consider the 365 cm^{-1} vibrational mode. The continuous lines represent fittings of the data in terms of (2) in the temperature range 20–140 K

the mean effective vibrational frequencies in the upper and ground electronic states, can assume values larger or smaller than unity; a red shift on increasing the temperature (hemoglobin derivatives) implies R less than unity, while a blue shift (myoglobin derivatives) implies R greater than unity (see also Table 2).

A final comment concerns the use of the Poisson distribution [see Eq. (1)] to take into account the fine structure of the high frequency vibrational modes. Indeed, Eq. (1) strictly holds for very low temperature; its use in the whole temperature range is based on the assumption that only the ground vibrational state is occupied even at 300 K. For the modes at 676 and 1374 cm^{-1}, because of the low value (typically <0.2) of the coupling constants S_j, this assumption appears to be well founded, while it is not strictly justified for the 365 cm^{-1} mode (whose $\langle n \rangle \approx 0.21$ at 300 K), because of the rather larger value of the coupling constant (0.6÷0.9).

In order to clarify if and how the thermal population of the 365 cm^{-1} mode affects the broadening and peak shift of the band, we have fitted (1) to our data without explicitly considering coupling of the electron transition with the 365 cm^{-1} vibrational mode, i.e. by considering this mode as belonging to the thermal bath; we stress, however, that the fittings of the spectra in the above approximation exhibit a larger (by a factor 3) χ^2 values at all temperatures with respect to the fitting reported in the Data Analysis section. The parameters σ^2 and v_0 resulting from this analysis in the case of HoMbCN are reported in Fig. 6 as a function of temperature and compared with the same

quantities already reported in Figs. 3 and 5. Data clearly indicate that, although larger σ_{in} and different $\nu_{00}+C$ values are induced, the population of the 365 cm^{-1} mode does not sizably affect the temperature dependent broadening and peak position shift of the band.

Acknowledgements. We wish to thank Dr. E. Vitrano for useful discussions and comments, and Mr. G. Lapis for technical help. This work was supported by grants from the Ministero dell'Università e della Ricerca Scientifica e Tecnologica (MURST) and from Comitato Regionale Ricerca Nucleare e Struttura della Materia (CRRNSM).

References

Ansari A, Berendzen J, Braunstein D, Cowen BR, Frauenfelder H, Hong MK, Iben IET, Johnson JB, Ormos P, Sauke TB, Scholl R, Schulte A, Steinbach PJ, Vittitow J, Young RD (1987) Rebinding and relaxation in the myoglobin pocket. Biophys Chem 26:337–355

Asher SA (1981) Resonance Raman spectroscopy of hemoglobin. Methods Enzymol 76:371–413

Bevington PR, Robinson DK (1992) Data reduction and error analysis for the physical sciences, 2nd edn. McGraw-Hill, New York

Boffi A, Verzili D, Chiancone E, Leone M, Cupane A, Militello V, Vitrano E, Cordone L, Yu W, Di Iorio EE (1994) Ligand binding kinetics and optical absorption spectra in the cooperative homodimeric scapharca inaequivalvis hemoglobin. Effect of protein fluctuations. Biophys J 67:1713–1723

Chan CK, Page JB (1983) Temperature effects in the time correlator theory of resonance raman scattering. J Chem Phys 79: 5234–5250

Cordone L, Cupane A, San Biagio PL, Vitrano E (1979) Effect of some monohydric alcohols on the oxygen affinity of hemoglobin: relevance of solvent dielectric constant and hydrophobicity. Biopolymers 18:1975–1988

Cordone L, Cupane A, Leone M, Vitrano E (1986) Optical absorption spectra of deoxy- and oxyhemoglobin in the temperature range 300-20 K: relation with protein dynamics. Biophys Chem 24:259–275

Cordone L, Cupane A, Leone M, Vitrano E, Bulone D (1988) Interaction between external medium and haem pocket in myoglobin probed by low-temperature optical specroscopy. J Mol Biol 198:213–218

Cordone L, Cupane A, Leone M, Vitrano E (1990) Thermal behaviour of the 760 nm absorption band in photodissociated sperm whale carbonmonoxy-myoglobin at cryogenic temperature: dependence on external medium. Biopolymers 29:639–643

Craig JM, Senge MO, Smith KM, Sparks LD, Shelnutt JA (1992) Nonplanar distortion modes for highly substituted porphyrins. J Am Chem Soc 114:9859–9869

Cupane A, Leone M, Vitrano E, Cordone L (1988) Structural and dynamic properties of the heme pocket in myoglobin probes by optical spectroscopy. Biopolymers 27:1977–1997

Cupane A, Leone M, Vitrano E (1993a) Protein dynamics: conformational disorder, vibrational coupling and anharmonicity in deoxyhemoglobin and myoglobin. Eur Biophys J 21:385–391

Cupane A, Leone M, Vitrano E, Cordone L, Hiltpold UR, Winterhalter KH, Yu W, Di Iorio EE (1993b) Structure-dynamics-function relationships in Asian Elephant (*Elephas maximus*) myoglobin. An optical spectroscopy and flash-photolysis study on functionally important motions. Biophys J 65:2461–2472

Cupane A, Leone M, Vitrano E, Cordone L (1995) Low temperature optical absorption spectroscopy: an approach to the study of stereodynamic properties of hemeproteins. Eur Biophys J 23:385–398

Desbois A, Lutz M, Banarjee R (1979) Low-frequency vibrations in resonance Raman spectra of horse heart myoglobin. Iron-ligand and iron-nitrogen vibrational modes. Biochemistry 18:1510–1518

Di Iorio EE, Hiltpold UR, Filipovic D, Winterhalter KH, Gratton E, Vitrano E, Cupane A, Leone M, Cordone L (1991) Protein dynamics: Comparative investigation on heme-proteins with different physiological roles. Biophys J 59:742–754

Di Pace A, Cupane A, Leone M, Vitrano E, Cordone L (1992) Vibrational coupling, spectral broadening mechanisms and anharmonicity effects in carbonmonoxy heme proteins studied by the temperature dependence of the Soret band lineshape. Biophys J 63:475–484

Eaton WA, Hofrichter J (1981) Polarized absorption and linear dichroism spectroscopy of hemoglobin. Methods Enzymol 76: 175–261

Eaton WA, Hanson LK, Stephens PJ, Sutherland JC, Dunn JBR (1978) Optical spectra of oxy- and deoxyhemoglobin. J Am Chem Soc 100:4991–5003

Frauenfelder H, Parak F, Young RD (1988) Conformational substates in proteins. Annu Rev Biophys Biophys Chem 17:451–479

Gilch H, Schweitzer-Stenner R, Dreybrodt W (1993) Structural heterogeneity of the Fe^{2+}-N_ε (His F8) band in various hemoglobin and myoglobin derivatives probed by the Raman-active iron histidine stretching mode. Biophys J 65:1470–1485

Gilch H, Dreybrodt W, Schweitzer-Stenner R (1995) Temperature dependence of the Fe-N_ε (His F8) Raman-band of deoxymyoglobin in aqueous solution. Biophys J (in press)

Jaffe' HH, Orchin M (1970) Theory and applications of ultraviolet spectroscopy, V edn, Wiley, New York

Leone M, Cupane A, Vitrano E, Cordone L (1987) Dynamic properties of oxy- and carbonmonoxyhemoglobin probed by optical spectroscopy in the temperature range 300-20 K. Biopolymers 26:1769–1779

Leone M, Cupane A, Vitrano E, Cordone L (1992) Strong vibronic coupling in heme proteins. Biophys Chem 42:111–115

Leone M, Cupane A, Cordone L (1994) Thermal broadening of the Soret band in heme complexes and in heme-proteins: role of iron dynamics. Eur Biophys J 23:349–352

Li X-Y, Czernuszewicz RS, Kincaid JR, Su YO, Spiro TG (1990) Consistent porphyrin force field. 1. Normal-mode analysis for nickel porphine and nickel tetraphenylporphine from resonance Raman and infrared spectra and isotope shifts. J Phys Chem 94:31–47

Machinen MW, Churg AK (1983) Structural and analytical aspects of the electronic spectra of hemeproteins. In: Lever IABP, Gray HB (eds) Iron porphyrins. Addison-Wesley, Reading Mass, pp 141–235

Marquardt DW (1963) An algorithm for least-squares estimation of non linear parameters. J Soc Ind Appl Math 11:431–441

Moffat K, Deatherage JF, Seybert DW (1979) A structural model for the kinetic behavior of hemoglobin. Science 206:1035–1042

Myers AB, Mathies RA, Tannor DJ, Heller EJ (1982) Excited state geometry changes from preresonance Raman intensity: isoprene and hexatriene. J Chem Phys 15:3857–3866

Schomacker KT, Champion PM (1986) Investigations of Spectral broadening Mechanisms in Biomolecules: Cytochrome-C. J Chem Phys 84:5314–5325

Schomacker KT, Bangcharoenpaurpong O, Champion PM (1984) Investigations of the stokes and anti-Stokes resonance Raman scattering of cytochome-C. J Chem Phys 80:4701–4717

Shelnutt JA, Medforth CJ, Berber MD, Barkigia KM, Smith KM (1991) Relationship between structural parameters and Raman frequencies for some planar and nonplanar nickel(II) porphyrins. J Am Chem Soc 113:4077–4087

Spiro TG (1983) The resonance raman spectroscopy of metallo porphyrins and heme proteins. In: Lever ABP, Gray HB (eds) Iron porphyrins II. Addison Wesley, Reading, Mass, pp 89–159

Srajer V, Champion PM (1991) Investigations of optical line shapes and kinetic hole burning in myoglobin. Biochemistry 30:7390–7402

Stavrov SS (1993) The effect of iron displacement out of the porphyrin plane on the resonance Raman spectra of heme proteins and iron porphyrins. Biophys J 65:1942–1950